Luminescent Heterobimetallic Complexes. Electronic Structure, Spectroscopy, and Photochemistry of $[AuPt(dppm)_2(CN)_2]ClO_4$ and the X-ray Crystal Structure of $[AgPt(dppm)_2(CN)_2(CF_3SO_3)]$

Hon-Kay Yip,[†] Hsui-Mei Lin,[‡] Kung-Kai Cheung,[†] Chi-Ming Che,*[,†] and Yu Wang[‡]

Departments of Chemistry, The University of Hong Kong, Pokfulam Road, Hong Kong, and The National Taiwan University, Taipei, Taiwan

Received July 28, 1993[⊛]

The d^{10}–d^8 heterobimetallic complexes $[AuPt(dppm)_2(CN)_2]ClO_4$ and $[AgPt(dppm)_2(CN)_2(CF_3SO_3)]$ (dppm = bis(diphenylphosphino)methane) were prepared by literature methods. The X-ray crystal structure of $[AgPt(dppm)_2(CN)_2(CF_3SO_3)]$ has been determined. Crystal data for $[AgPt(dppm)_2(CN)_2(CF_3SO_3)]$: monoclinic, space group $P2_1$, $a = 10.453(2)$ Å, $b = 16.372(4)$ Å, $c = 14.846(6)$ Å, and $\beta = 92.17(2)°$. The intramolecular Pt···Ag distance is 3.002(1) Å. The absorption spectra of $[AuPt(dppm)_2(CN)_2]ClO_4$ and $[AgPt(dppm)_2(CN)_2(CF_3SO_3)]$ exhibit intense $^1(d\sigma^* \rightarrow p\sigma)$ transitions at 323 nm and 317 nm, respectively. The results of extended Hückel molecular orbital calculations suggested that the $d\sigma^*$ orbital in each case is mainly composed of the Pt ($5d_{z^2}$) orbital. In acetonitrile and at room temperature, $[AuPt(dppm)_2(CN)_2]ClO_4$ exhibits a broad emission (lifetime = 18 μs) at 570 nm. The emitting state has been suggested to be $^3(d\delta^*p\sigma)$. The effect of solvent on the emission properties has been investigated. The $[AgPt(dppm)_2(CN)_2(CF_3SO_3)]$ complex shows metal-perturbed intraligand emission in glass solution at 77 K. The rate constants of quenching of the excited state of $[AuPt(dppm)_2(CN)_2]^+$ by pyridinium acceptors have been treated by Marcus quadratic, Rehn–Weller, and Agmon–Levine equations and the excited state reduction potential of $[AuPt(dppm)_2(CN)_2]^+$, $[Au–Pt]^{2+} + e^- \rightarrow [Au–Pt]^{+*}$, is estimated to be about −1.73 to −1.80 V vs SCE. The photoreactions of $[AuPt(dppm)_2(CN)_2]^+$ with halocarbons were investigated by Stern–Volmer quenching, flash photolysis, and steady-state photolysis experiments. An electron transfer mechanism is suggested.

Introduction

In the last two decades, the spectroscopy and photochemistry of luminescent homodinuclear d^8–d^8 complexes like $[Pt_2(P_2O_5H_2)_4]^{4-}$ [1a] and $[Rh_2(1,3\text{-diisocyanopropane})_4]^{2+}$ [1b] and d^{10}–d^{10} complexes such as $[M_2(dppm)_3]$ (M = Pt(0) and Pd(0)) [1c] and $[Au_2(dppm)_2]^{2+}$ (dppm = bis(diphenylphosphino)methane) [1d–f] have been investigated intensively with regard to their spectroscopic and photochemical properties. Related studies on luminescent heterobimetallic complexes[2] are still in their infancy. In this context, Balch and co-workers have done some interesting studies on $[IrAu(dppm)_2(CO)(Cl)]^+$ [2a] and various Ir–Tl [2b] and Pt–Tl complexes.[2c] The spectroscopic properties of some d^{10}–main group ions have also been reported by Fackler and co-workers recently.[2d] It is our purpose to further explore the photochemistry of heterobimetallic complexes and recently we have communicated the structure and spectroscopic properties of a d^{10}–d^8 complex, $[AuPt(dppm)_2(CN)_2]ClO_4$,[3] which has been shown to have an emissive and long-lived electronic excited state in fluid solution at room temperature. In this work, the spectroscopy and crystal analysis of another d^{10}–d^8 complex, $[AgPt(dppm)_2(CN)_2(CF_3SO_3)]$ as well as further spectroscopic and photochemical investigations of $[AuPt(dppm)_2(CN)_2]ClO_4$ are described. A direct comparison between the electronic absorption spectra of $[AuPt(dppm)_2(CN)_2]^+$ and $[AgPt(dppm)_2(CN)_2(CF_3SO_3)]$ with that of the related homodinuclear d^8–d^8 *trans*-$[Pt_2(dppm)_2(CN)_4]$ complex[4] is also presented.

Experimental Section

Materials. The pyridinium salts,[5] $[AuPt(dppm)_2(CN)_2]ClO_4$,[6a] and *trans*-$[Pt(dppm)_2(CN)_2]$,[6a] were synthesized by literature procedures. $Na[Co(EDTA)]$ was synthesized by reacting $CoCl_2$ (0.3 g) sodium acetate (0.05 g), and EDTA (ethylenediaminetetraacetic acid) (0.67 g) in boiling water for $^1/_2$ h. Addition of acetone to the solution gave 1 deep purple solid which was purified by recrystallization in ethanol. The halocarbons used in the Stern–Volmer experiments were purified according to the literature methods.

Synthesis. $[AgPt(dppm)_2(CN)_2(CF_3SO_3)]$. A dichloromethane solution (20 mL) of $AgCF_3SO_3$ (0.05 g, 0.2 mmol) and *trans*-$[Pt(dppm)_2(CN)_2]$ (0.2 g, 0.2 mmol) was stirred for 30 min and filtered. Upon addition of diethyl ether, a white precipitate was obtained. The crude product was recrystallized by diffusing diethyl ether into a dichloromethane solution. The structure of the complex was established by X-ray crystal analysis.

Steady-State Photolysis. A solution of $[AuPt(dppm)_2(CN)_2]ClO_4$ (0.3 g) and *n*-butyl iodide (0.3 mL) in acetonitrile (100 mL) was degassed by purging with N_2 in quartz tubes for 30 min. The solution was irradiated with a mercury lamp equipped with a water jacket to cut off the high UV for about 2 h. The inorganic product(s) was (were) precipitated from the resulting solution by addition of diethyl ether.

Molecular Orbital Calculations. Extended Huckel molecular orbital (EHMO) calculations were made on $[AuPt(dmpm)_2(CN)_2]^+$ and $[AgPt(dppm)_2(CN)_2(CF_3SO_3)]$ (dmpm = bis(dimethylphosphino)methane).

[†] The University of Hong Kong.
[‡] The National Taiwan University.
[⊛] Abstract published in *Advance ACS Abstracts,* March 1, 1994.

(1) (a) Roundhill, D. M.; Gray, H. B.; Che, C.-M. *Acc. Chem. Res.* **1989**, *22*, 55. (b) Mann, K. R.; Gordon, J. G. II; Gray, H. B. *J. Am. Chem. Soc.* **1975**, *97*, 3553. (c) Harvey, P. D.; Gray, H. B. *J. Am. Chem. Soc.* **1988**, *110*, 2145. (d) Che, C.-M.; Kwong, H. L.; Poon, C.-K.; Yam, V. W.-W. *J. Chem. Soc. Dalton Trans.* **1990**, 3215. (e) Che, C.-M.; Kwong, H. L.; Yam, V. W.-W.; Cho, C.-K. *J. Chem. Soc., Chem. Commun.* **1989**, 885. (f) King, C.; Wang, J.-C.; Khan, N. I. Md.; Fackler, J. P., Jr.; *Inorg. Chem.* **1989**, *28*, 2145.
(2) (a) Balch, A. L.; Catalano, V. J.; Olmstead, M. M. *Inorg. Chem.* **1990**, *29*, 585. (b) Balch, A. L.; Neve, F.; Olmstead, M. M. *J. Am. Chem. Soc.* **1991**, *113*, 2995. (c) Nagle, J. K.; Balch, A. L.; Olmstead, M. M. *J. Am. Chem. Soc.* **1988**, *110*, 319. (d) Wang, S.; Grazon, G.; King, C.; Wang, J.-C.; Fackler, J. P., Jr. *Inorg. Chem.* **1989**, *28*, 4623.
(3) Yip, H.-K.; Che, C.-M.; Peng, S.-M. *J. Chem. Soc., Chem. Commun.* **1991**, 1626.
(4) Che, C.-M.; Yam, V. W.-W.; Wong, W. T.; Lai, T.-F. *Inorg. Chem.* **1989**, *28*, 758.
(5) Kwong, H. L. M. Phil. Thesis The University of Hong Kong, 1989.
(6) (a) Hassan, F. S. M.; Markham, D. P.; Pringle, P. G.; Shaw, B. L. *J. Chem. Soc., Dalton Trans.* **1985**, 279. (b) Langrick, C. R.; McEwan, D. M.; Pringle, P. G.; Shaw, B. L. *J. Chem. Soc., Dalton Trans.* **1983**, 2487. (c) Cooper, G. R.; Hutton, A. T.; Langrick, C. R.; McEwan, D. M.; Pringle, P. G.; Shaw, B. L. *J. Chem. Soc., Dalton Trans.* **1984**, 855.

0020-1669/94/1333-1644$04.50/0 © 1994 American Chemical Society

Table 1. Crystallographic Data for $[AgPt(dppm)_2(CN)_2(CF_3SO_3)]$

fw = 1272.87	space group: monoclinic, $P2_1$
a = 10.453(2) Å	λ = 0.710 73 Å
b = 16.372(4) Å	ρ_{calcd} = 1.665 g cm^{-3}
c = 14.846(6) Å	μ(Mo Kα) = 33.8 cm^{-1}
β = 92.17(2)°	$R(F_o)$ = 0.049
V = 2538.8(1.0) Å^3	$R_w(F_o)$ = 0.057
Z = 2	
T = 23 ± 1 °C	

The geometry of both species was taken from X-ray diffraction data with all the phenyl groups on P replaced by methyl groups. EHMO calculations were carried out using ICON program.[7] The H_{ii}, ξ values for Au,[8] Pt,[9] and Ag[10] were taken from the literature.

Instruments. UV–vis absorption spectra were recorded on a Milton Roy Spectronic 3000 diode array spectrophotometer. Emission spectra were recorded on a Spex Fluorolog-2 spectrofluorometer. Infrared spectra were obtained as Nujol mull on a Nicolet 20SX FT-IR spectrometer. ^{1}H NMR spectra were recorded on a Jeol GSX 270-MHz spectrometer with TMS used as standard. The experimental setup for emission lifetime and transient absorption experiments had been described elsewhere.[1d] Emission quantum yield was measured in degassed solution with [Ru(2,2′-bipyridine)$_3$](ClO$_4$)$_2$ as the reference.[11]

X-ray Crystal Structure of $PtAg(C_{25}H_{22}P_2)_2(CN)_2{\cdot}CF_3SO_3$. X-ray diffraction data were collected at 23 °C on a Enraf-Nonius CAD-4 diffractometer with graphite monochromatized Mo Kα radiation (λ = 0.710 73 Å). The complex crystallizes out in thin plates and the crystals are yellow. A crystal of dimensions 0.05 × 0.15 × 0.25 mm was used for using ω–2θ scan with ω-scan angles (0.60 + 0.344 tan θ)° at scan speeds of 1.37–5.49 deg min^{-1}. Intensity data (in the range of $2\theta_{max}$ = 50°; h = 0 to 12; k = 0 to 19; l = −17 to 17) were corrected for Lorentz and polarization effects and empirical absorption based on the ψ-scan of four strong reflections. Crystallographic data are summarized in Table 1. Upon averaging of the 5452 reflections, 5162 independent reflections were obtained. 3821 reflections with $F_o \geq 3\sigma(F_o)$ were considered observed and used in the structural analysis. From systematic absences, the space group can be $P2_1$ or $P2_1/m$. Since the molecule does not contain a mirror plane, the alternate space group P $2_1/m$ can be ruled out. The structure was solved by Patterson and Fourier methods and refined by full-matrix least-squares methods using the Enraf-Nonius SDP-1985 programs on a MicroVAX II computer. The 48 phenyl carbon atoms were refined isotropically and the other 18 Pt, Ag, S, F, O, N, and C atoms were refined anisotropically and H atoms at calculated positions and isotropic thermal parameters equal to 1.3 times that of the attached C atoms were not refined. Convergence for 362 variables by least square refinement with $w = 4F^2/\sigma^2(F_o^2)$ where $\sigma^2(F_o^2) = [\sigma^2(I) + (0.04F_o^2)^2]$ was reached at R = 0.049, R_w = 0.057, and S = 1.466 for the 3821 reflections. $(\Delta/\sigma)_{max}$ = 0.03. Refinement of the enantiomorp converges at R = 0.058, R_w = 0.070, S = 1.543, and $(\Delta/\sigma)_{max}$ = 0.04. A final difference Fourier map was featureless, with maximum positive and negative peaks of 2.0 and 2.5 e Å^{-3} respectively. Table 2 lists the atomic coordinates of non-hydrogen atoms. Selected bond distances and angles are given in Table 3.

Results and Discussion

The syntheses and characterization of a variety of dppm-bridged heterobimetallic (e.g. d^{10}–d^8, d^8–d^8, and d^8–d^6) complexes were established by Shaws and co-workers since early 1980s.[6] Their physical and chemical properties, however, only received little attention until recently we and Balch independently reported the photoluminescent properties of some d^{10}–d^8 [2a,3] and d^8–d^8 [12] complexes. Most of the heterobimetallic complexes studied by Balch and co-workers[2a,12a] have short emission lifetimes in fluid solution at room temperature. The $[AuPt(dppm)_2(CN)_2]^+$ complex described in this work presents an exceptional opportunity to explore the photochemistry of the heterobimetallic complexes because of its intriguing long excited state lifetime.

Table 2. Positional Parameters and Their Estimated Standard Deviations for $[AgPt(dppm)_2(CN)_2(CF_3SO_3)]$

atom	x	y	z	B,[a] Å^2
Pt	0.32024(5)	0.250	0.88510(4)	2.152(8)
Ag	0.4219(1)	0.15853(8)	0.72779(8)	2.87(2)
S	0.7222(4)	0.2505(5)	0.6412(3)	4.15(8)
P(1)	0.4348(4)	0.1594(3)	0.9775(3)	2.31(7)
P(2)	0.1953(4)	0.3295(2)	0.7865(3)	2.26(8)
P(3)	0.4544(4)	0.0385(2)	0.8225(3)	2.36(8)
P(4)	0.2563(4)	0.2184(3)	0.6274(3)	2.52(8)
F(1)	0.602(2)	0.212(1)	0.490(1)	12.6(5)
F(2)	0.689(2)	0.112(1)	0.563(1)	12.9(6)
F(3)	0.806(2)	0.195(1)	0.491(1)	13.4(5)
O(1)	0.831(1)	0.2146(9)	0.687(1)	5.6(3)
O(2)	0.609(1)	0.2407(9)	0.6883(9)	5.6(3)
O(3)	0.739(2)	0.3311(9)	0.604(1)	7.5(4)
N(1)	0.117(1)	0.110(1)	0.852(1)	5.1(4)
N(2)	0.505(1)	0.3934(9)	0.941(1)	4.6(4)
C(1)	0.191(1)	0.161(1)	0.862(1)	2.8(3)
C(2)	0.440(1)	0.342(1)	0.9177(9)	2.6(3)
C(3)	0.409(1)	0.055(1)	0.939(1)	2.8(3)*
C(4)	0.132(1)	0.2698(9)	0.6915(9)	2.9(3)*
C(5)	0.376(1)	0.166(1)	1.092(1)	3.0(3)*
C(6)	0.253(2)	0.133(1)	1.104(1)	5.2(5)*
C(7)	0.202(3)	0.142(2)	1.195(2)	8.3(7)*
C(3)	0.274(2)	0.181(2)	1.258(2)	6.6(6)*
C(9)	0.388(2)	0.215(1)	1.244(1)	5.5(5)*
C(10)	0.438(2)	0.207(1)	1.159(1)	4.3(4)*
C(11)	0.609(1)	0.166(1)	0.991(1)	2.8(3)*
C(12)	0.678(2)	0.212(1)	0.935(1)	3.3(3)*
C(13)	0.813(2)	0.205(1)	0.940(1)	4.5(4)*
C(14)	0.869(2)	0.153(1)	1.001(1)	4.9(4)*
C(15)	0.801(2)	0.107(1)	1.057(1)	5.3(5)*
C(16)	0.667(2)	0.111(1)	7.049(1)	3.4(3)*
C(17)	0.052(1)	0.3697(9)	0.8393(9)	2.4(3)*
C(18)	−0.061(2)	0.375(1)	0.789(1)	4.1(4)*
C(19)	−0.167(2)	0.407(1)	0.833(1)	4.8(4)*
C(20)	−0.160(2)	0.430(1)	0.917(1)	4.4(4)*
C(21)	−0.049(2)	0.426(2)	0.967(1)	6.0(5)*
C(22)	0.064(2)	0.395(1)	0.927(1)	4.6(4)*
C(23)	0.272(2)	0.417(1)	0.737(1)	3.7(4)*
C(24)	0.400(2)	0.420(2)	0.731(1)	6.1(5)*
C(25)	0.459(3)	0.486(2)	0.690(2)	7.2(6)*
C(26)	0.391(2)	0.553(2)	0.664(2)	6.5(6)*
C(27)	0.265(3)	0.554(2)	0.678(2)	7.6(6)*
C(28)	0.198(2)	0.484(1)	0.710(1)	5.2(4)*
C(29)	0.615(1)	−0.0013(9)	0.826(1)	2.5(3)*
C(30)	0.648(2)	−0.079(1)	0.857(1)	3.5(3)*
C(31)	0.772(2)	−0.108(1)	0.854(1)	5.7(5)*
C(32)	0.865(2)	−0.055(1)	0.824(1)	5.2(5)*
C(33)	0.827(2)	0.021(1)	0.795(1)	4.7(4)*
C(34)	0.714(2)	0.046(1)	0.796(1)	3.8(4)*
C(35)	0.351(2)	−0.047(1)	0.786(1)	3.2(3)*
C(36)	0.318(2)	−0.108(1)	0.345(1)	4.3(4)*
C(37)	0.242(2)	−0.173(1)	0.817(1)	5.0(4)*
C(38)	0.214(2)	−0.178(1)	0.726(1)	6.0(5)*
C(39)	0.251(2)	−0.122(2)	0.667(2)	7.0(6)*
C(40)	0.324(2)	−0.057(1)	0.697(1)	4.5(4)*
C(41)	0.280(1)	0.292(1)	0.536(1)	2.9(3)*
C(42)	0.179(2)	0.306(1)	0.476(1)	4.4(4)*
C(43)	0.197(2)	0.364(2)	0.405(1)	6.1(5)*
C(44)	0.309(2)	0.401(2)	0.402(2)	6.6(6)*
C(45)	0.409(2)	0.388(2)	0.459(2)	6.5(5)*
C(46)	0.394(2)	0.331(1)	0.530(1)	4.3(4)*
C(47)	0.177(2)	0.133(1)	0.569(1)	3.2(3)*
C(48)	0.061(2)	0.105(1)	0.585(1)	4.4(4)*
C(49)	0.009(2)	0.038(2)	0.538(2)	7.3(6)*
C(50)	0.085(2)	−0.002(2)	0.479(2)	6.6(6)*
C(51)	0.205(2)	0.024(1)	0.461(1)	5.7(5)*
C(52)	0.248(2)	0.091(1)	0.509(1)	5.2(5)*
C(53)	0.701(3)	0.192(2)	0.537(2)	8.8(8)

[a] Values marked with an asterisk denote atoms that were refined isotorpically. Values for anisotropically refined atoms are given in the form of the isotropic equivalent displcement parameter defined as $(4/3)[a^2B(1,1) + b^2B(2,2) + c^2B(3,3) + ab(\cos\gamma)B(1,2) + ac(\cos\beta)B(1,3) + bc(\cos\alpha)B(2,3)]$.

(7) Howell, J.; Rossi, A.; Wallacer, D.; Haraki, K.; Hoffmann, R. ICON programs. Quantum Chemistry Program Exchange, 1977.
(8) Janiak, C.; Hoffman, R. *Inorg. Chem.* **1989**, *28*, 2743.
(9) Schilling, B. E. R.; Hoffman, R. *J. Am. Chem. Soc.* **1979**, *101*, 3456.
(10) Jorgenson, K.; Hoffman, R. *J. Phys. Chem.* **1990**, *94*, 3046.
(11) Demas, J. N.; Crosby, G. A. *J. Phys. Chem.* **1971**, *75*, 991.
(12) (a) Balch, A. L.; Catalano, V. J. *Inorg. Chem.* **1992**, *31*, 3934. (b) Yip, H.-K.; Lin, S.-M.; Wang, Y.; Che, C.-M. *Inorg. Chem.* **1993**, *32*, 3402.

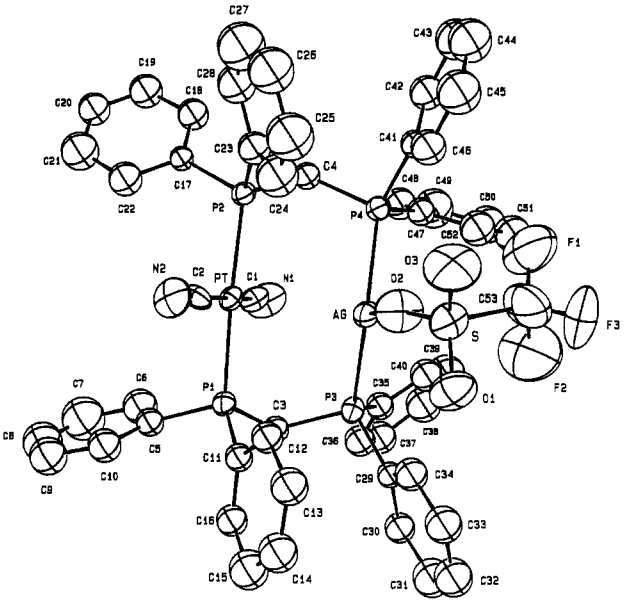

Figure 1. Perspective view of $[AgPt(dppm)_2(CN)_2(CN)_2(CF_3SO_3)]$.

Table 3. Selected Bond Lengths (Å) and Angles (deg) of $[AgPt(dppm)_2(CN)_2(CF_3SO_3)]$

Pt–Ag	3.002(1)	Pt–P(1)	2.322(4)
Pt–P	2.323(4)	Ag–P(3)	2.433(4)
Ag–P(4)	2.446(4)	Pt–C(1)	2.00(2)
Pt–C(2)	2.00(2)	Ag–O(2)	2.46(1)
C(1)–Pt–C(2)	174.7(6)	P(1)–Pt–P(2)	174.3(1)
P(3)–Ag–P(4)	139.2(1)	O(2)–Ag–P(3)	118.9(3)
O(2)–Ag–P(4)	100.7(3)	P(1)–Pt–C(1)	88.1(5)
P(1)–Pt–C(2)	91.9(4)	P(2)–Pt–C(1)	86.6(5)
P(2)–Pt–C(2)	93.6(4)		

X-ray Crystal Structure of $[AgPt(dppm)_2(CN)_2(CF_3SO_3)]$. A perspective view of $[AgPt(dppm)_2(CN)_2(CF_3SO_3)]$ is shown in Figure 1. The structure is different from that of $[AuPt(dppm)_2(CN)_2]^+$, which has been communicated recently.[3] Instead of being in C_{2v} symmetry, it has a C_1 symmetry. Similar to the case of $[Ag_2(dppm)_2(NO_3)_2]$,[13] the $CF_3SO_3^-$ is weakly coordinated to the Ag ion, which is in a distorted trigonal planar geometry with P–Ag–P angle of 139.2(1)° and O–Ag–P angles of 118.9(3) and 100.7(3)°. The coordination geometry of Pt is closely square planar, similar to that in $[AuPt(dppm)_2(CN)_2]^+$.[3] The Pt–Ag distance of 3.002(1) Å is comparable to the Pt–Au (3.046(2) Å) distance found in $[AuPt(dppm)_2(CN)_2]^+$.[3] On the other hand, the intramolecular metal–metal distance in the related homodinuclear d^8–d^8 complex *trans*-$[Pt_2(dppm)_2(CN)_4]$ has been previously reported to be 3.301(1) Å,[4] which is much longer than the respective Pt–Au and Pt–Ag distances of $[AuPt(dppm)_2(CN)_2]^+$ and $[AgPt(dppm)_2(CN)_2(CF_3SO_3)]$.

Electronic Spectra and Molecular Orbital Calculation.

Figure 2 displays the absorption spectra of $[AuPt(dppm)_2(CN)_2]ClO_4$ and $[AgPt(dppm)_2(CN)_2(CF_3SO_3)]$ measured in acetonitrile. The absorption spectrum of $[AuPt(dppm)_2(CN)_2]ClO_4$ is dominated by the intense absorptions at 323 nm (ϵ_{max} = 1.32×10^4 M^{-1} cm^{-1}) and 270 nm (ϵ_{max} = 1.21×10^4 M^{-1} cm^{-1}). Besides, a weak absorption ($\epsilon \approx 500$ M^{-1} cm^{-1}) appears around 360–410 nm. The 323-nm band highly resembles to the $^1(d\sigma^* \rightarrow p\sigma)$ transitions of the d^8–d^8 complexes studied by Gray and others[1a,b] and hence may be assigned to it. Indeed, Balch and co-workers[2a] had assigned the lowest energy allowed transition of another d^{10}–d^8 complex, $[AuIr(dppm)_2(CO)Cl]^+$, to the $^1(d\sigma^* \rightarrow p\sigma)$ transition. However, the spectral assignment of $[AuPt(dppm)_2(CN)_2]^+$ is not as simple as it appears to be. As shown in the figure, $[AgPt(dppm)_2(CN)_2(CF_3SO_3)]$ exhibits an intense

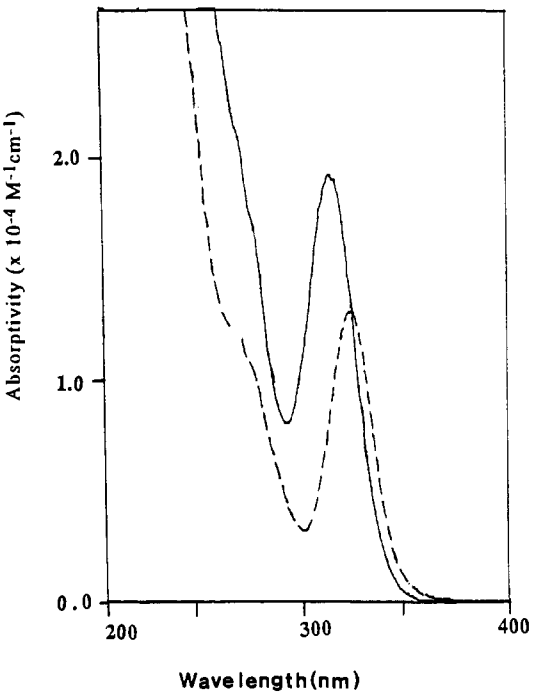

Figure 2. Absorption spectra of $[AgPt(dppm)_2(CN)_2(CF_3SO_3)]$ (—) and $[AuPt(dppm)_2(CN)_2]ClO_4$ (- - -) in acetonitrile at 298 K.

absorption band at 317 nm (ϵ_{max} = 1.93×10^4 M^{-1} cm^{-1}), which is close in energy to the proposed $^1(d\sigma^* \rightarrow p\sigma)$ transition of $[AuPt(dppm)_2(CN)_2]^+$ at 323 nm. It is interesting to note that the related homodinuclear d^8–d^8 *trans*-$[Pt_2(dppm)_2(CN)_4]$ complex, which has an intramolecular Pt–Pt separation of 3.301(1) Å, also has the $^1(d\sigma^* \rightarrow p\sigma)$ transition located at similar energy (324 nm).[4]

In order to understand these UV–vis spectral data, EHMO calculations on the model complexes, $[AuPt(dmpm)_2(CN)_2]^+$, $[AgPt(dmpm)_2(CN)_2(CF_3SO_3)]$, and *trans*-$[Pt_2(dmpm)_2(CN)_4]$ (dmpm = bis(dimethylphosphino)methane) have been performed and the results are given in Figure 3. The results indicate that the $d\sigma^*$ orbital in each case mainly arises from the antibonding interaction of the two metal valence d_{z^2} orbitals. However, for the heterobimetallic Pt–Au or Pt–Ag systems, the contributions of the $5d_{z^2}$ of Au or $4d_{z^2}$ of Ag to $d\sigma^*$ is small. The coefficients of $5d_{z^2}$ (Pt) in the $d\sigma^*$ orbitals of $[AuPt(dmpm)_2(CN)_2]^+$ and $[AgPt(dmpm)_2(CN)_2(CF_3SO_3)]$ are 0.487 and 0.553, respectively, whereas that of $5d_{z^2}$ (Au) and $4d_{z^2}$ (Ag) are –0.196 and –0.216, respectively. The $p\sigma$ orbitals have significant contribution from the $6p_z$ orbital of Pt and π^* orbitals of CN in both complexes. Given the small contribution of the Au(I) or Ag(I) in the $d\sigma^*$ and $p\sigma$ orbitals of the complexes, these orbitals should be mainly derived from the *trans*-$[Pt(dppm)_2(CN)_4]$ moiety. It may be more appropriate to describe the $d\sigma^* \rightarrow p\sigma$ transition to be a metal perturbed $Pt(5d_{z^2}) \rightarrow (6p_z, \pi^*)$ charge transfer transition. The calculated difference in energies between the $d\sigma^*$ and $p\sigma$ orbitals are 29 079 cm^{-1} and 27 933 cm^{-1} for $[AuPt(dppm)_2(CN)_2]^+$ and $[AgPt(dppm)_2(CN)_2(CF_3SO_3)]$, respectively. The difference between these two values is very small, in line with the observation that the lowest energy dipole-allowed electronic transitions of the two complexes have similar λ_{max} values. For *trans*-$[Pt_2(dppm)_2(CN)_4]$, the HOMO, alike other homodinuclear d^8–d^8 complexes, is a $d\sigma^*$ orbital which is almost entirely made up of the Pt $(5d_{z^2})$ orbitals. The LUMO, $p\sigma$, on the other hand, is composed of the $Pt(6p_z)$ and π^* orbitals of cyanides and phosphorous. The coefficients of both $6p_z$ orbitals in the $p\sigma$ are about 0.22 while those of the π^* of the cyanides are 0.17–0.25. The results suggest that the $d\sigma^* \rightarrow p\sigma$ transition has significant charge transfer character. Thus, the 324-nm band of *trans*-$[Pt_2(dppm)_2(CN)_4]$, previously labeled as $^1(d\sigma^* \rightarrow p\sigma)$,[4] may also be

(13) Ho, D. M.; Bau, R. *Inorg. Chem.* **1983**, *22*, 4073.

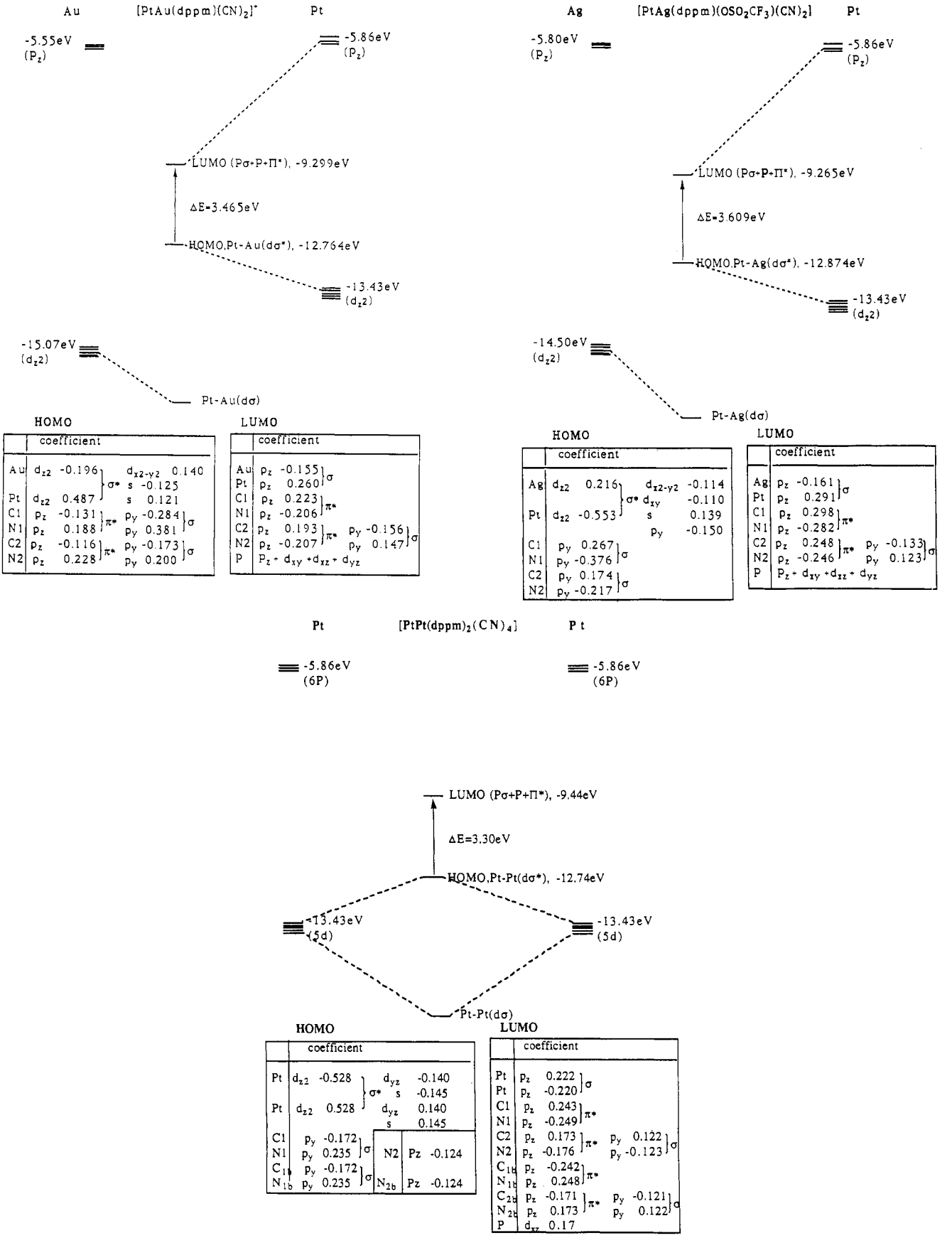

Figure 3. Molecular orbital diagrams for (a, top left) $[AuPt(dmpm)_2(CN)_2]^+$, (b, top right) $[AgPt(dmpm)_2(CN)_2(CF_3SO_3)]$, and (c, bottom) *trans*-$[Pt_2(dmpm)_2(CN)_2]$.

regarded as a Pt(II)-perturbed MLCT transition of the mononuclear *trans*-$Pt(dppm)_2(CN)_2$ moiety.

Photophysical and Luminescent Properties. Upon excitation of $[AuPt(dppm)_2(CN)_2]ClO_4$ at 350 nm in acetonitrile, a broad emission (full width at half-height = 3950 cm^{-1}) centered at 570 nm is observed, as shown in Figure 4. The emission quantum yield and lifetime, which were found to be relatively insensitive to the complex concentration, are 0.02 and 18 μs, respectively.[3]

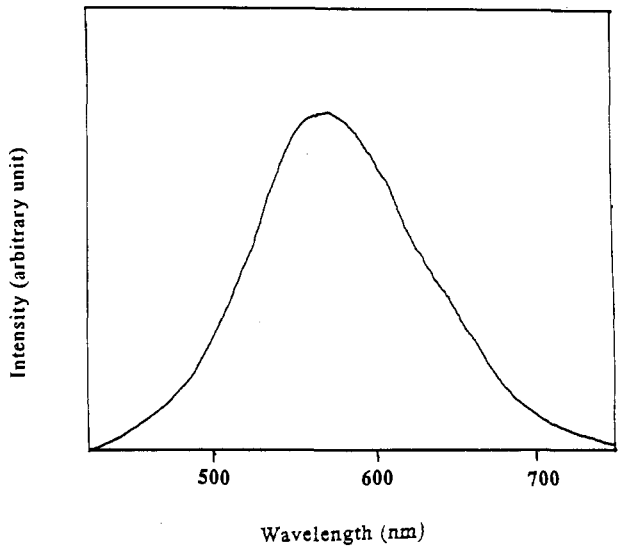

Figure 4. Emission psectrum of a degassed acetonitrile solution of $[AuPt(dppm)_2(CN)_2]ClO_4$ at 298 K (excited at 350 nm).

Table 4. Photophysical Data for $[AuPt(dppm)_2(CN)_2]X$

solvents	lifetime, μs	quantum yield
acetonitrile, X = ClO_4^-	18.0	0.02
ethanol, X = Cl^-	9.8	0.009
methanol, X = Cl^-	7.5	0.009
1,2-dichloroethane, X = $CF_3SO_3^-$	16.2	0.015

The photophysical properties measured in other solvents are listed in Table 4. Notably, the emission energy does not vary with the solvents, but the lifetime and quantum yield are lower in alcoholic solvents than in 1,2-dichloroethane and acetonitrile. The shorter emission lifetime and lower quantum yield in 1,2-dichloroethane may be due to the oxidative quenching by the solvent since $[AuPt(dppm)_2(CN)_2]^+$ has been found to be a powerful photoreductant (see later section). It is interesting to find that the Stokes shift between the maxima of the emission and $^1(d\sigma^* \rightarrow p\sigma)$ transition is exceptionally large (13 415 cm^{-1}). It is apparent that the 570-nm emission of $[AuPt(dppm)_2(CN)_2]^+$ is unlikely to come from the $^3(d\sigma^*p\sigma)$ excited state.

The anomalous emission of $[AuPt(dppm)_2(CN)_2]^+$ is rather similar to those of polynuclear Au(I) complexes such as $[Au_2(dppm)_2]^{2+}$ where broad emission bands and large Stokes shifts between the $^1(d\sigma^* \rightarrow p\sigma)$ transition and the emission have been found. For the polynuclear Au(I) complexes the lowest electronic excited state has been suggested to be $^3(d\delta^*p\sigma)$.[1d] It is probable that the emitting excited state of $[AuPt(dppm)_2(CN)_2]^+$ is also $^3(d\delta^*p\sigma)$ in nature, where the $d\delta^*$ orbital is mainly composed of the $5d_{x^2-y^2}$ orbital of Au. However, attempts to locate the $d\delta^* \rightarrow p\sigma$ transition of the complex have so far been unsuccessful.

Figure 5 depicts the emission spectrum of $[AuPt(dppm)_2(CN)_2]ClO_4$ measured in *n*-butyronitrile glass solution at 77 K. The emission spectrum, which has a sharp and intense emission band at 435 nm and a less intense and broad emission at 550 nm, is distinctly different from that recorded at room temperature. A similar emission spectrum has also been found in a 77 K MeOH/EtOH (1:4, v/v) glass solution. The 435-nm emission is absent at room temperature. According to previous photophysical studies of arylphosphines,[14] the 435-nm emission is tentatively assigned to the $^3(\pi^* \rightarrow \pi)$ transition of dppm. From the 77 K emission spectrum, the E_{0-0} (energy of 0–0 transition) of the excited state of $[AuPt(dppm)_2(CN)_2]^+$ is estimated at ~450 nm (2.8 eV).

While $[AgPt(dppm)_2(CN)_2(CF_3SO_3)]$ displays no emission either in dichloromethane or solid state at room temperature, a

(14) (a) Fife, D. J.; Morse, W. M.; Morse, K. W. *Inorg. Chem.* **1984**, *23*, 1545. (b) Segers, D. P.; DeArmond, M. K.; Grutsch, P. A.; Kutal, C. *Inorg. Chem.* **1984**, *23*, 2874.

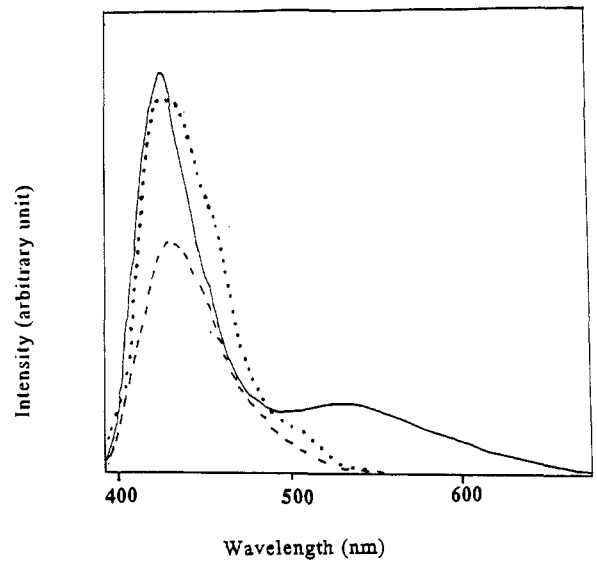

Figure 5. Emission spectra of 77 K *n*-butyronitrile glass solutions of $[AuPt(dppm)_2(CN)_2]ClO_4$ (—), $[AgPt(dppm)_2(CN)_2(CF_3SO_3)]$ (- - -), and dppm (···).

Table 5. Rate Constants for the Quenching of the Emission of $[AuPt(dppm)_2(CN)_2]ClO_4$ by the Pyridinium Acceptors in 0.1 M $[NBu_4]PF_6$ Acetonitrile Solution at 298 K

quencher[a]	$E(Q^+/Q^0)$,[b] V	$10^{-9}k_{q'}$,[c] $dm^3\ mol^{-1}\ s^{-1}$
4-cyano-*N*-methylpyridinium	–0.67	21.70
4-methoxycarbonyl-*N*-methylpyridinium	–0.78	14.52
4-amino-*N*-methylpyridinium	–0.93	4.40
3-amino-*N*-ethylpyridinium	–1.14	0.88
N-ethylpyridinium	–1.36	0.13
4-methyl-*N*-methylpyridinium	–1.49	0.013
2,6-dimethyl-*N*-methylpyridinium	–1.52	0.004

[a] All the pyridinium acceptors are hexafluorophosphate salts. [b] Potential quoted vs saturated calomel electrode (SCE). [c] $k_{q'}$ is the rate constant corrected for the diffusion rate constant which is estimated to be $1 \times 10^{10}\ dm^3\ mol^{-1}\ s^{-1}$.

n-butyronitrile glass solution of the complex at 77 K exhibits an emission at 435 nm (Figure 5), which can be tentatively assigned to intraligand in nature.

Photoreactions with Pyridinium Acceptors. The long excited-state lifetime of $[AuPt(dppm)_2(CN)_2]^+$ makes the complex attractive for photochemical study. Since the complex displays no reduction or oxidation wave (in the range 1.5 to –1.2 V vs $Ag/AgNO_3$) in acetonitrile during cyclic voltammetric scans, it is not possible to estimate the excited state reduction potential from spectroscopic data. Rather this was established by studying the quenching of the emission by a series of pyridinium acceptors.

Results of the study are summarized in Table 5. All the quenching reactions obey Stern–Volmer kinetics and are electron transfer in nature (eq 1).

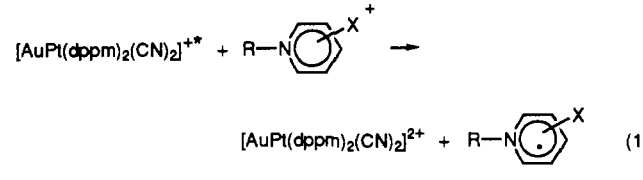

(1)

Spectroscopic evidence for the pyridinium radical has been obtained through flash photolysis experiments. The transient difference absorption spectrum recorded at 20 μs after flashing a degassed acetonitrile solution of $[AuPt(dppm)_2(CN)_2]ClO_4$ and methyl viologen (MV^{2+}) is close to the reported spectrum of MV^+ (Figure 6).[15] All the transient signals were found to decay

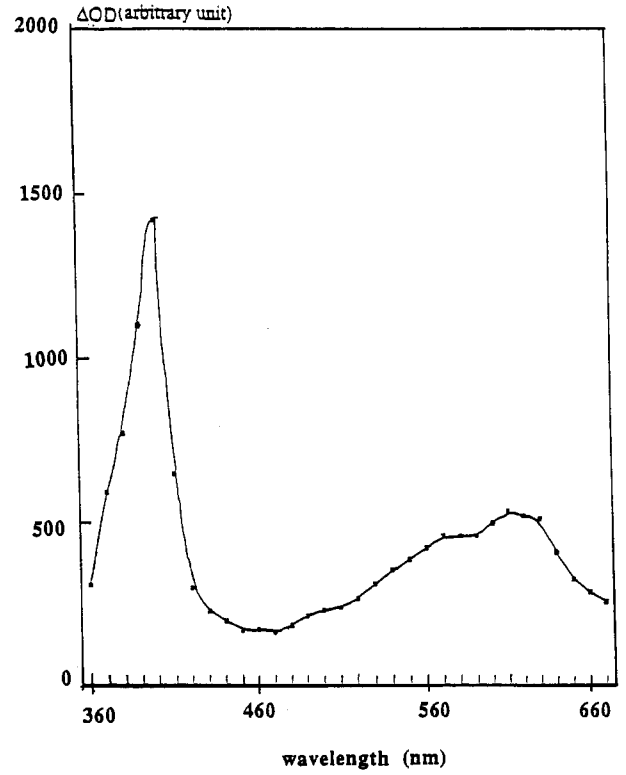

Figure 6. Transient difference absorption spectrum obtained at 20 μs after laser flash photolysis of a degassed acetonitrile solution of $[AuPt(dppm)_2(CN)_2]ClO_4$ (2.1×10^{-4} M) and methylviologen hexafluorophosphate (1.3×10^{-3} M).

Table 6. Excited-State Reduction Potential, $E(Pt–Au^{2+}/Pt–Au^{+*})$ and Total Reorganization Energy for the Electron Transfer Reaction (λ) from Three-Parameter Nonlinear Least-Squares Fits to the Marcus Quadratic, Rehm–Weller, and Agmon–Levine Equations

equations	$E(Pt–Au^{2+}/Pt–Au^{+*})$, V *vs* SCE	λ, eV
Marcus quadratic	−1.80 ± 0.03	0.90 ± 0.03
Rehm–Weller	−1.73 ± 0.02	0.85 ± 0.01
Agmon–Levine	−1.78 ± 0.02	0.92 ± 0.01

back to the level before the laser flash and second-order kinetics was found for the decay. This is consistent with the facile back-electron-transfer of $[AuPt(dppm)_2(CN)_2]^{2+}$ and MV^+ to give the starting $[AuPt(dppm)_2(CN)_2]^+$ and MV^{2+} (eq 2).

$$[AuPt(dppm)_2(CN)_2]^{2+} + MV^+ \rightarrow [AuPt(dppm)_2(CN)_2]^+ + MV^{2+} \quad (2)$$

Fitting the transient decay trace at 610 nm gave second-order kinetics with a rate constant of 1.1×10^9 M^{-1} s^{-1} for the back-reaction.

The quenching rate constants and the reduction potentials of the pyridinium acceptors were fitted with the Marcus quadratic,[16] Rehm–Weller,[17] and Agmon–Levine[18] equations, and the results obtained from the fittings are listed in Table 6. The $E(Pt–Au^{2+}/Pt–Au^{+*})$ value of the reaction

$$[AuPt(dppm)_2(CN)_2]^{2+} + e^- \rightarrow [AuPt(dppm)_2(CN)_2]^{+*}$$

obtained from the fittings ranges from −1.73 to −1.80 V (vs SCE), indicating that $[AuPt(dppm)_2(CN)_2]^+$ is a powerful photoreductant. Similar excited state reduction potentials have also been found in the polynuclear gold(I) phosphine complexes such as $[Au_2(dppm)_2]^{2+}$, $[Au_2(dmpm)_2]^{2+}$ (dmpm = bis(dimethylphosphino)methane),[1d] and $[Au_3(dppp)_2]^{3+}$ (dppp = bis(diphenylphosphino)phenylmethane) (−1.6 V vs SCE).[19] The total reorganization energy λ of the reaction (eq 3), ranging from 0.85

$$\lambda = \lambda_{in} + \lambda_{out} \quad (3)$$

V to 0.91 V, is also comparable to those found in the related electron transfer reactions of the $^3(d\delta^*p\sigma)$ excited state of $[Au_2(dppm)_2]^{2+}$ [1d] and $^3(d\sigma^*p\sigma)$ excited state of $[Ir_2(Pyz)_2(COD)_2]$ (PyzH = pyrazole; COD = 1,5-cyclooctadiene) (0.85 eV).[20] The outer-sphere reorganization energy, λ_{out}, for the electron transfer reaction between the $[AuPt(dppm)_2(CN)_2]^{+*}$ and pyridinium acceptors can be calculated by eq 4, in which the reactants are treated as spheres and the solvent as a dielectric continuum.[16,21]

$$\lambda_{out} = \frac{\Delta e}{4\pi\epsilon_0}\left(\frac{1}{2r(Au-Pt^{+*})} + \frac{1}{2r(Q^+)} - \frac{1}{r_{ab}}\right)\left(\frac{1}{\epsilon_{op}} - \frac{1}{\epsilon_s}\right) \quad (4)$$

The calculated λ_{out} is 0.83 eV. It is therefore clear that the λ for the reaction represented by equation 1 is dominated by λ_{out}. Given the similar radii of the $[Au_2(dppm)_2]^{2+}$ and $[AuPt(dppm)_2(CN)_2]^+$ cations, it is expected that the two complexes should have similar λ_{out} values. This accounts for the similar λ values of the two systems. Similarly the λ of the reaction between the excited state of $[Ir_2(pyz)_2(COD)_2]$ and pyridinium acceptors was suggested by Gray and co-workers[20] to arise mainly from the solvent reorganization energy, λ_{out}, of acetonitrile. From the excited state reduction potential and E_{0-0}, the reduction potential of the reaction

$$[AuPt(dppm)_2(CN)_2]^{2+} + e^- \rightarrow [AuPt(dppm)_2(CN)_2]^+ \quad (5)$$

is estimated to be +1 V vs SCE. Thus the species $[AuPt(dppm)_2(CN)_2]^{2+}$ is a strong oxidant. Attempts have been tried to isolate $[AuPt(dppm)_2(CN)_2]^{2+}$, but these were unsuccessful. Its optical spectrum, however, has been characterized by oxidative quenching of the excited state of $[AuPt(dppm)_2(CN)_2]^+$ with O_2 and $[Co^{III}(EDTA)]^-$. Figure 7 shows the transient difference absorption spectrum recorded at 10 μs after laser flashing an aerated acetonitrile solution of $[AuPt(dppm)_2(CN)_2]ClO_4$. The 570 nm emission of the complex (lifetime < 20 ns in aerated acetonitrile) is largely quenched by oxygen. It is expected that the highly reducing excited state of the complex is capable to react with oxygen via an electron transfer process. The transient signal of the oxygen quenching reaction is weak, and the transient spectrum shown in Figure 7 is suggested to come from the $[AuPt(dppm)_2(CN)_2]^{2+}$ cation. This argument is supported by the similar difference absorption spectrum recorded upon flashing a degassed acetonitrile solution of $[AuPt(dppm)_2(CN)_2]ClO_4$ and $[Co^{III}(EDTA)]^-$.

Photoreactions with Halocarbons. Apart from the pyridinium acceptors, the emission of $[AuPt(dppm)_2(CN)_2]^+$ is also quenched by halocarbons. Table 7 summarizes the results of the quenching studies. The correlation between the quenching rate constants (k_q) with $D(C–X)$ is not good. For example, the C–Cl dissociation energies of benzyl chloride and carbon tetrachloride differ by 1 kcal/mol but the respective quenching rate constants

(15) Kosower, E. M.; Cotter, J. L. *J. Am. Chem. Soc.* **1964**, *86*, 5524.
(16) Marcus, R. A.; Sutin, N. *Biochim. Biophys. Acta* **1985**, *811*, 265.
(17) Rehm, D.; Weller, A. *Isr. J. Chem.* **1970**, *8*, 259.
(18) Agmon, N.; Levine, R. D. *Chem. Phys. Lett.* **1977**, *52*, 197.
(19) Yam, V. W.-W.; Lai, T.-F.; Che, C.-M. *J. Chem. Soc., Dalton Trans.* **1990**, 3747.
(20) McCleskey, T. M.; Winkler, J. R.; Gray, H. B. *J. Am. Chem. Soc.* **1992**, *114*, 6935.
(21) The $r(Au–Pt^{+*})$ and $r(Q^+)$ are the radii of the excited state complex and pyridinum acceptors. It is assumed that the complex has similar radii in both its excited state and ground state. From X-ray crystal data, the radii of $[AuPt(dppm)_2(CN)_2]^+$ is estimated to be about 8 Å. The radii of the pyridinium acceptors are estimated to be about 4 Å. r_{ab} is the center-to-center separation of between the two reactants and is taken to be the sum of their radii, that is 12 Å. Δe is the charge transferred in the reaction and is equal to one electron charge. ϵ_0, ϵ_{op}, and ϵ_s are the vacuum permittivity, optical dielectric, and static dielectric constants of acetonitrile, respectively.

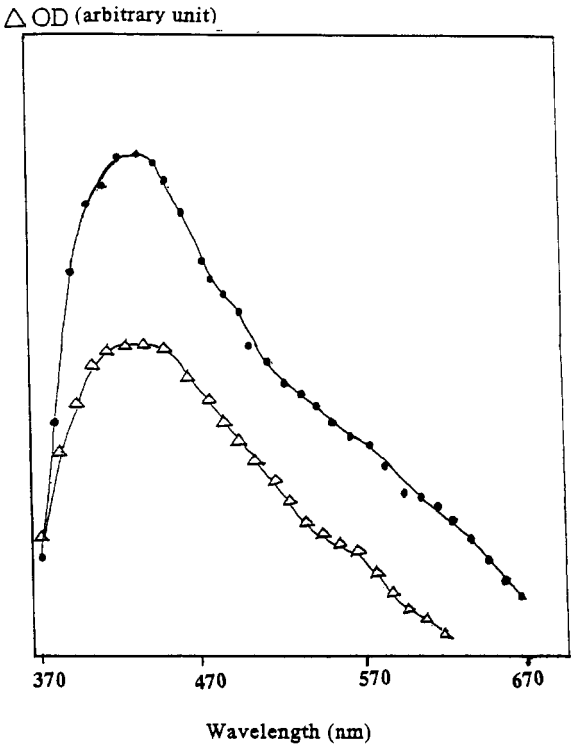

Figure 7. Transient difference absorption spectra obtained at 10 μs after laser flash photolysis of an aerated acetonitrile solution of $[AuPt(dppm)_2(CN)_2]ClO_4$ (3.5×10^{-4} M, •) and Na[Co(EDTA)] (2.5×10^{-3} M, △).

Table 7. Rate Constants for the Quenching of the Emission of $[AuPt(dppm)_2(CN)_2]ClO_4$ by Halocarbons in Degassed Acetonitrile Solution at 298 K

halocarbons	$10^{-9}k_{q'}$,[a] M^{-1} s^{-1}	$-E_{1/2}$ of RX,[b] V	D(C–X),[c] kcal mol^{-1}
CBr_4	6.02	0.30	56
$CHBr_3$	5.52	0.64	56
CCl_4	1.10	0.68	70
CH_2=CHBr	0.93	1.21	55
$C_6H_5CH_2Br$	0.61	1.36	55
$BrCH_2CH_2Br$	0.075	1.52	
CH_3I	1.01	1.63	53
CH_3CH_2I	0.92	1.67	
n-C_4H_9I	1.13		
$CHCl_3$	0.051	1.67	78
$C_6H_5CH_2Cl$	0.0024	1.97	69

[a] Rate constants are corrected with the diffusion rate constant estimated as 2×10^{10} M^{-1} s^{-1}. [b] Half-wave potentials were measured in 75% dioxane/25% water against SCE: Mann, C. K.; Barnes, K. K. *Electrochemical Reactions in Nonaqueous Systems*: Marcel Dekker, Inc.: New York, 1970. [c] *CRC Handbook of Chemistry and Physics*: West, R. C., Ed.; CRC Press, Inc.: Boca Raton, FL, 1985.

are different by 3 orders of magnitude. Figure 8 shows the plot of ln $k_{q'}$ vs the half-wave reduction potential of the halocarbons. A trend of increasing $k_{q'}$ accompanying the increase of $E_{1/2}$(RX) is apparent and hence an electron transfer mechanism is suggested (eq 6). Significant deviations from the trend are the alkyl iodides, which display exceptionally large quenching rate constants.

$$[AuPt(dppm)_2(CN)_2]^{+*} + RX \rightarrow [AuPt(dppm)_2(CN)_2]^{2+} + RX^{\bullet -} \quad (6)$$

In order to elucidate the mechanism of quenching, flash photolysis experiments were performed. Figure 9 shows the transient difference spectra recorded at 10 μs after flashing (at 355 nm) degassed acetonitrile solutions of $[AuPt(dppm)_2(CN)_2]ClO_4$ containing benzyl chloride and *n*-butyl bromide, respectively. The two spectral profiles are very similar to that of $[AuPt(dppm)_2(CN)_2]^{2+}$ which could also be generated by the photoreaction of

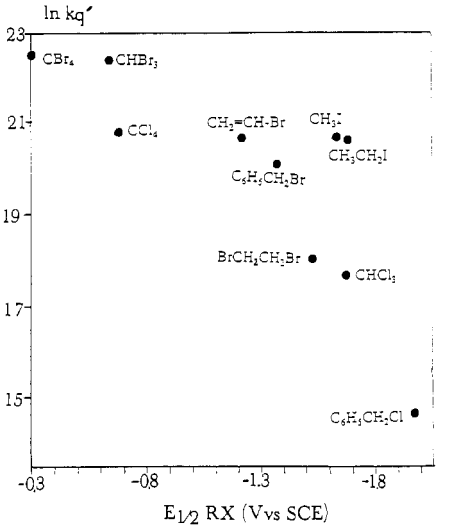

Figure 8. Plot of quenching rate constant ($k_{q'}$) of the reactions of the excited state of $[AuPt(dppm)_2(CN)_2]^+$ and the halocarbons *vs* half-wave reduction potentials of the halocarbons.

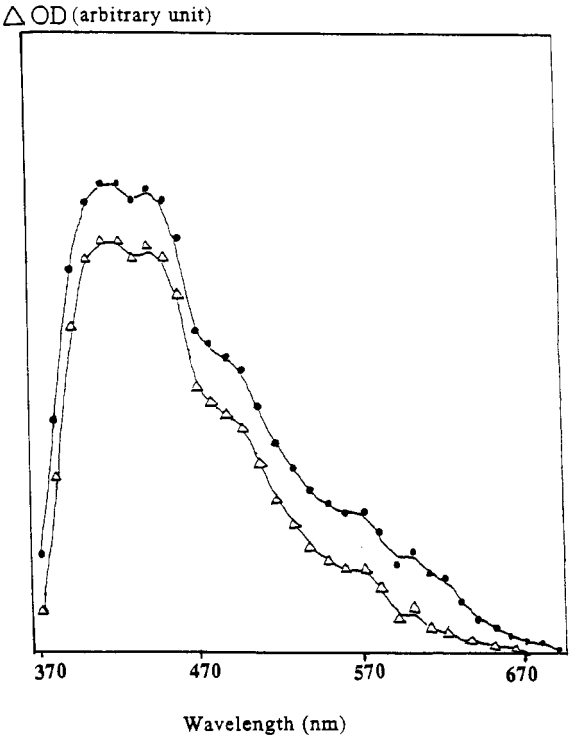

Figure 9. Transient difference absorption spectra obtained at 10 μs after laser flash photolysis of a degassed acetonitrile solution of $[AuPt(dppm)_2(CN)_2]ClO_4$ (2.8×10^{-4} M) and benzyl chloride (3.5×10^{-3} M, •) and *n*-butyl bromide (2.7×10^{-3} M, △).

the complex with oxygen or $[Co^{III}(EDTA)]^-$ (Figure 7). If an intermediate containing metal-halide bond was formed in the photochemical reaction, (eq 7), it is reasonable to expect that the

$$[AuPt(dppm)_2(CN)_2]^{+*} + RX \rightarrow [AuPt(dppm)_2(CN)_2(X)]^{+} + R^{\bullet} \quad (7)$$

two absorption spectra would be different. The result of flash photolysis experiment is in favor of eq 6.

Steady-state photolysis experiments have been performed. With alkyl chlorides and benzyl chloride, no detectable photoreaction was observed within minutes. Figure 10 shows the spectral trace of the photoreaction of $[AuPt(dppm)_2(CN)_2]ClO_4$ with *n*-butyl iodide in degassed acetonitrile (excitation = 350

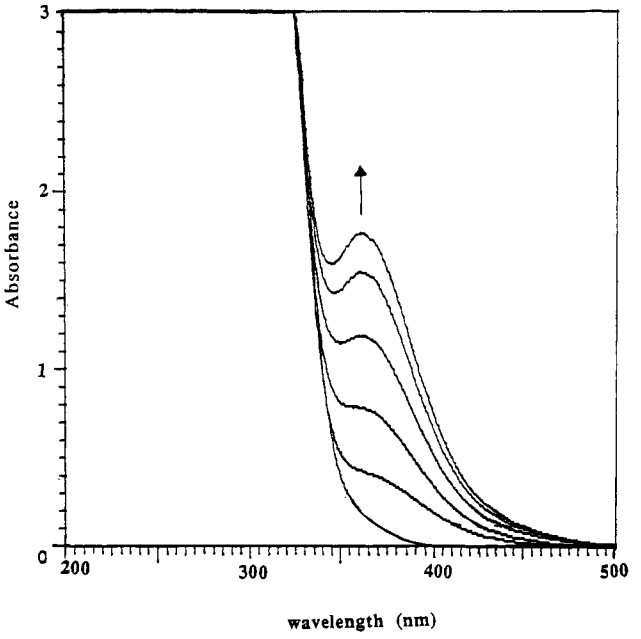

Figure 10. Absorption spectral change during steady photolysis (irradiated at 350 nm) of a degassed acetonitrile solution of $[AuPt(dppm)_2(CN)_2]ClO_4$ and *n*-butyl iodide (time interval ~ 1 min).

nm). The photoreaction is completed within 10 min. As shown in the figure, a new species having absorption at 363 nm is formed during the reaction. The 363-nm absorption band is due to *cis*-$[Pt(dppm)I_2]$, which had been isolated after photolysis and had its structure identified by x-ray crystal analysis (see experimental section). Because the excited state of $[AuPt(dppm)_2(CN)_2]^+$ is a powerful reductant, the primary step of the photoreaction would be eq 8. It is suggested that the initially generated $[AuPt(dppm)_2(CN)_2]^{2+}$ species with a $E(Au\text{–}Pt^{2+}/Au\text{–}Pt^{+})$ value of +1 V vs SCE may undergo oxidative cleavage reaction with the coordinated cyanide. Oxidative cleavage of the Pd–C bond had been

$$[AuPt(dppm)_2(CN)_2]^{+*} + n\text{-BuI} \rightarrow [AuPt(dppm)_2(CN)_2]^{2+} + [n\text{-BuI}]^{\bullet -} \quad (8)$$

observed in the case of *cis*-$[Pd(dmpe)(R)_2]$ (dmpe = bis(dimethylphosphino)ethane; R = alkyl) by Trogler and coworkers.[22]

General Comments. From this study, the $^1(d\sigma^* \rightarrow p\sigma)$ transitions of the heterobimetallic complexes $[AuPt(dppm)_2(CN)_2]^+$ and $[AgPt(dppm)_2(CN)_2(CF_3SO_3)]$ have substantial contribution from the MLCT transition of the P–$Pt(CN)_2$–P moiety. This is different from the $^1(d\sigma^* \rightarrow p\sigma)$ transitions of $[Pt_2(P_2O_5H_2)_4]^{4-}$ and $[Rh_2(1,3\text{-diisocyanopropane})_4]^{2+}$, which are shown to be highly metal localized.

In contrast to the $^3(d\sigma^*p\sigma)$ state of $[Pt_2(P_2O_5H_2)_4]^{4-}$, which reacts with halocarbons via an atom transfer mechanism, the quenching of the excited state of $[AuPt(dppm)_2(CN)_2]^+$ by halocarbons is charge transfer in nature. The difference would be due to the different nature of the excited states of the complexes. The $^3(d\sigma^*p\sigma)$ excited state of $[Pt_2(P_2O_5H_2)_4]^{4-}$ is diradical-like and consists of two unpaired electrons in the "exposed" $d\sigma^*$ and $p\sigma$ orbitals.[23] This favours the orbital overlap between the complex and halocarbons, which is essential for the atom transfer process. On the contrary, the excited state of $[AuPt(dppm)_2(CN)_2]^+$ is suggested to be $^3(d\delta^*p\sigma)$ in nature. Especially, the $p\sigma$ orbital of this complex is not as metal-localized as the one in $[Pt_2(P_2O_5H_2)_4]^{4-}$, and this renders the photoinduced atom transfer reaction less facile.

Acknowledgment. We acknowledge support from the Hong Kong Research Council and the Croucher Foundation of Hong Kong. C.M.C. is thankful for a visiting professorship, administered by National Taiwan University.

Supplementary Material Available: Tables of positional parameters for hydrogen atoms, bond distances and bond angles, and general displacement parameter expressions (4 pages). Ordering information is given on any current masthead page.

(22) Seligson, A. L.; Trogler, W. C. *J. Am. Chem. Soc.* **1992**, *114*, 7085.
(23) Smith, D. C.; Gray, H. B. *Coord. Chem. Rev.* **1990**, *100*, 169.